

Magnetic penetration depth in single-crystal $\text{YBa}_2\text{Cu}_3\text{O}_{7-\delta}$

D. R. Harshman, L. F. Schneemeyer, J. V. Waszczak, G. Aeppli,*
R. J. Cava, B. Batlogg, and L. W. Rupp
AT&T Bell Laboratories, Murray Hill, New Jersey 07974

E. J. Ansaldo

University of Saskatchewan, Saskatoon, Saskatchewan, Canada S7N 0W0

D. Li. Williams

University of British Columbia, Vancouver, British Columbia, Canada V6T 2A6

(Received 8 September 1988; revised manuscript received 1 November 1988)

We report the first measurement of the magnetic penetration depth $\lambda(T, \theta)$ in single crystals of $\text{YBa}_2\text{Cu}_3\text{O}_{7-\delta}$ ($\delta \sim 0.1$). Results are consistent with conventional s -wave pairing, and yield penetration depths of $\lambda_{ab}(0) = 1415 \pm 30 \text{ \AA}$ and $\lambda_c(0) > 7000 \text{ \AA}$, parallel and perpendicular to the basal plane, respectively. Comparative data on sintered $\text{YBa}_2\text{Cu}_3\text{O}_7$ are also shown to be consistent with the single-crystal results. The muon-spin-rotation data, together with specific-heat results, indicate a two-dimensional carrier density of $\eta_{2D} \approx 8 \times 10^{14} \text{ carriers cm}^{-2}$ and a basal-plane effective mass of $m_{ab}^*/m_e \approx 10$.

The magnetic penetration depth (λ), which measures the length over which magnetic fields are attenuated near the surface of a superconductor, is one of the most fundamental properties of superconductors. It is, therefore, not surprising that there is a rapidly increasing literature on λ for the new high- T_c superconductors.¹ Many techniques, most notably muon-spin-rotation (μ^+ SR), polarized neutron reflectometry, and ac susceptibility, have already been used to measure λ for the $R\text{-Ba-Cu-O}$ (R denotes rare earth) and $\text{La}_{2-x}\text{Sr}_x\text{CuO}_4$ superconductors.¹⁻³ Of particular relevance to the present work is an earlier μ^+ SR study² of sintered $\text{YBa}_2\text{Cu}_3\text{O}_{6.9}$, which provided the first evidence for conventional s -wave pairing in this material. Variations in the values of the penetration depth extracted from the various measurements on (nominally) equivalent materials have been attributed to the powdered nature and preparation differences of the specimens studied to date. In view of this and the extreme anisotropy of the copper-oxide based superconductors, a study of oriented single crystals is clearly desirable. To this end, we have performed the first measurements of the temperature- (T) and orientation- (θ) dependent penetration depth $\lambda(T, \theta)$ for single crystals of $\text{YBa}_2\text{Cu}_3\text{O}_{7-\delta}$.

The $\text{YBa}_2\text{Cu}_3\text{O}_{7-\delta}$ crystals were grown from a partially melting $\text{CuO-BaO-Y}_2\text{O}_3$ mixture and then annealed in oxygen, as described previously.⁴ The crystals grow as platelets with the c axis normal to the growth surfaces, and with significant microtwinning in the a - b plane. A relatively small oxygen deficiency ($\delta \sim 0.1$) was achieved by annealing the crystals for three weeks at 500°C in O_2 . The dc magnetization curve for these nearly stoichiometric ($\delta \sim 0.1$) crystals is shown (filled circles) in Fig. 1, along with corresponding data for oxygen-deficient ($0.3 \leq \delta \leq 0.4$) crystals and a fully stoichiometric ($\delta = 0$) sintered powder. The ($\delta \sim 0.1$) crystals, with typical dimensions $2 \times 2 \times 0.1 \text{ mm}^3$, were assembled into a flat mosaic sample, with the c axes aligned perpendicular to its

face, and mounted on 99.999% pure aluminum (high-purity aluminum exhibits no appreciable relaxation of the muon spin).

The time-differential μ^+ SR technique is described elsewhere,⁵ so only a brief description will be given here. Energetic (4.2 MeV) positive muons, produced at the TRIUMF Cyclotron, are stopped in the sample where they decay via the weak interaction $\mu^+ \rightarrow e^+ + \bar{\nu}_\mu + \nu_e$, emitting the positron preferentially along their final spin polarization direction. Since the muons are created with spins aligned opposite to their momentum, it is possible to follow the time evolution of the muon-spin direction after thermalizing in the sample; normally a clock is started when the muon enters the sample region, and stopped upon the subsequent detection of the decay positron. Each data point shown in the present work represents an

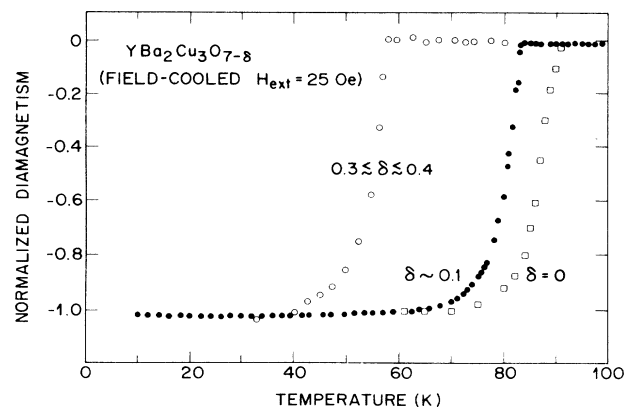


FIG. 1. dc magnetization ($H_{\text{ext}} = 25 \text{ Oe}$) measured in field-cooled sintered (squares) and single-crystal (circles) $\text{YBa}_2\text{Cu}_3\text{O}_{7-\delta}$. The filled circles correspond to $\delta \sim 0.1$ and the open circles to $0.3 \leq \delta \leq 0.4$.

ensemble average of $\sim 10^6$ such events. Only transverse-field geometry was used in the present work, where the magnetic field is applied perpendicular to the initial muon polarization. Such a configuration yields a spin-relaxation function $G_{xx}(t)$ consisting of a relaxation envelope which modulates a precessing muon amplitude. The experiments were conducted on field-cooled samples with the external field (>10 kG) applied along the initial beam momentum to help focus the incident muons onto the samples. In order to conform with transverse-field geometry, the muon spins were rotated perpendicular to their momentum using a crossed-field separator upstream of the sample.

Asymmetry spectra (in arbitrary units) for single-crystal $\text{YBa}_2\text{Cu}_3\text{O}_{7-\delta}$ ($\delta \sim 0.1$), taken with the field (11 kG) applied parallel ($\theta=0$) to the c axis, are shown in Fig. 2. For clarity and display, the data have been transformed to a rotating reference frame where the precession frequency is shifted by an amount corresponding to the muon precession frequency in the aluminum backing. Note that the data exhibit a full initial asymmetry, which is independent of temperature throughout the temperature range studied. The time-dependent relaxation function $G_{xx}(t)$ is essentially the Fourier transform of the internal field distribution $\rho(B)$ in the sample; slowly and rapidly decaying $G_{xx}(t)$'s correspond to narrow and broad distributions $\rho(B)$, respectively. Upon entering the (type II) superconducting state below T_c , the formation of the vortex lattice induces an inhomogeneous broadening in $\rho(B)$ and a concomitant increase in the decay rate of $G_{xx}(t)$, as can be seen in Fig. 2.

In our analysis of the single-crystal data, we approxi-

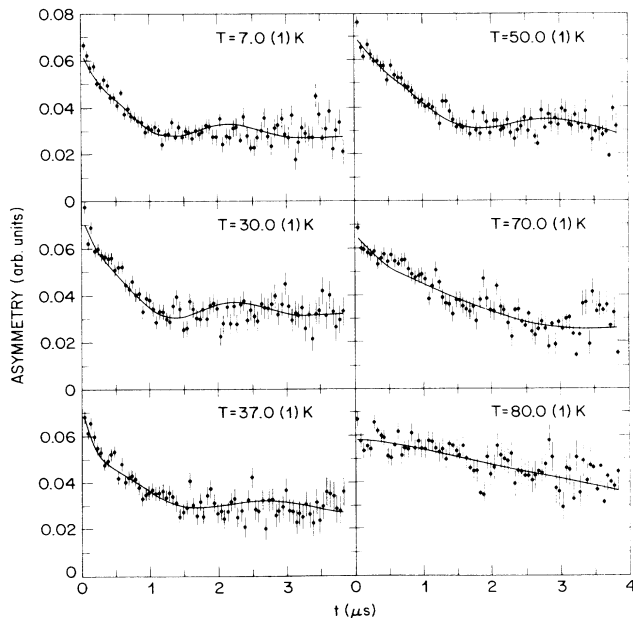


FIG. 2. Asymmetry spectra (plotted in the rotating reference frame) for single-crystal $\text{YBa}_2\text{Cu}_3\text{O}_{7-\delta}$, with $\delta \sim 0.1$. The curves are fits to the data assuming the line shape given in Eq. (1). All data shown here and in Fig. 3(a), except for that with $T=30$ K, were taken on field cooling.

mate⁶ the internal field distribution $\rho(B)$, associated with an Abrikosov flux lattice, by an exponential distribution with a cutoff at low fields. Within this model, $\rho(B)$ is defined as

$$\rho(B) = \begin{cases} \frac{1}{B_0} \exp\left[-\frac{(B-B_c)}{B_0}\right], & \text{for } B \geq B_c, \\ 0, & \text{for } B < B_c. \end{cases} \quad (1)$$

Here, B_c corresponds to the minimum strength of the field in the superconductor, while the exponential tail is due to the high fields near the vortex cores. Of course, the latter should be cutoff at high fields as well because of the finite-pair coherence length ξ ; we ignore this effect because of the extreme type-II nature of $\text{YBa}_2\text{Cu}_3\text{O}_{7-\delta}$. While Eq. (1) is not an exact expression for the field distribution, it is a simple analytical form which approximates existing numerical calculations⁷ of $\rho(B)$ better than either the Gaussian or Lorentzian line shapes used in the analysis of high- T_c data to date. The curves shown in Fig. 2 represent the best fits to the data assuming the form of Eq. (1), multiplied by a Gaussian function associated with nuclear dipolar fields.

For a perfect triangular vortex lattice, the width of the field distribution $\langle |\Delta B|^2 \rangle$ is related to the penetration depth λ via the asymptotic equation⁷

$$\langle |\Delta B|^2 \rangle = B_0^2 = 0.00371 \phi_0^2 \lambda^{-4}, \quad (2)$$

where ϕ_0 is the magnetic flux quantum ($=2.068 \times 10^{-7}$ G cm²). Note that the choice of lattice geometry (i.e., triangular versus square) introduces a small ($\sim 4\%$) variation in the calculated λ value. The resulting values of the hard-axis penetration depth $\lambda(T,0) = \lambda_{ab}(T)$ are plotted as a function of temperature in Fig. 3(a). As is evident, $\lambda(T,0)$ is independent of temperature below ~ 30 K, indicating consistency with conventional s -wave pairing, in agreement with earlier measurements² on sintered powders. For conventional superconductors, the temperature dependence of the magnetic penetration depth is well described by the equation

$$\lambda(T) = \lambda(0) \left[1 - \left(\frac{T}{T_c} \right)^4 \right]^{-1/2}. \quad (3)$$

Although Eq. (3) is a good approximation, it is not identical to the exact numerical calculation in which $\lambda(T)$ depends on individual material parameters such as the mean free path and coupling strength. The dashed curve in Fig. 3(a) is the fit to the data assuming the form of Eq. (3), which gives $\lambda_{ab}(0) = 1415 \pm 30$ Å, with a corresponding transition temperature of 82 ± 0.3 K. Infrared reflectivity data⁸ on crystals similar to those used in the present work, indicate a penetration depth (calculated from the oscillator-strength sum rule⁹) of $\lambda_{ab}^{\text{plasma}} \approx 1400$ Å [for the polarization in the basal (a - b) plane] that compares well with our μ^+ SR determination. Preliminary high-field (~ 18 kG) data on oxygen-deficient ($0.3 \lesssim \delta \lesssim 0.4$) single crystals (a typical dc-magnetization curve is shown in Fig. 1) indicate a $\lambda_{ab}(0)$ of 2550 ± 60 Å ($T_c \sim 65$ K), which is nearly twice that found for $\delta \sim 0.1$. This result has been substantiated by measurements⁶ on a single-phase sintered sample of $\text{YBa}_2\text{Cu}_3\text{O}_{6.77}$, and directly contradicts a

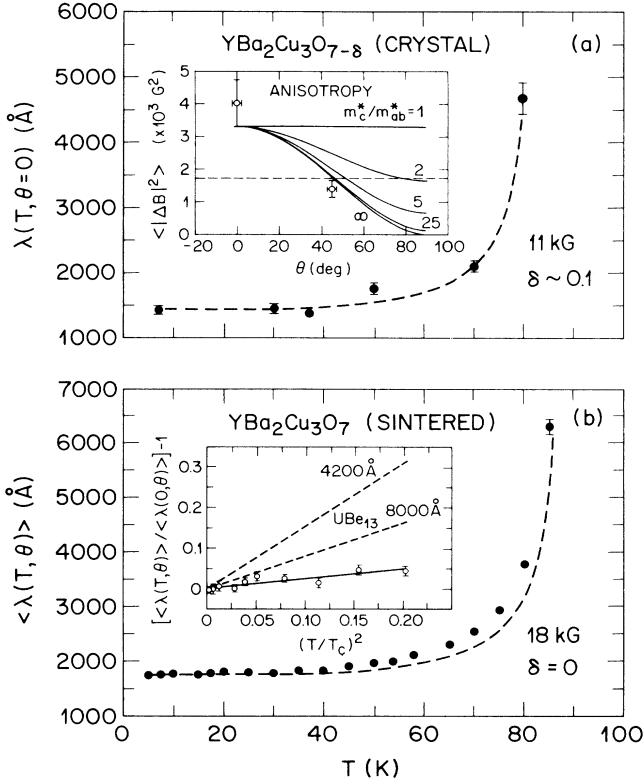


FIG. 3. The temperature dependence of (a) $\lambda(T, 0)$ in single-crystal $\text{YBa}_2\text{Cu}_3\text{O}_{7-\delta}$ ($\delta \sim 0.1$), and (b) $\langle \lambda(T, \theta) \rangle$ in sintered $\text{YBa}_2\text{Cu}_3\text{O}_7$. The dashed curves are fits to the data assuming Eq. (3). The inset in frame (a) shows $\langle |\Delta B|^2 \rangle$ as a function of θ (open circles), along with the expected behavior (solid curves) derived from Ref. 18. The dashed line represents the angle-averaged value. The inset in frame (b) shows the relative incremental penetration depth for $T \leq 40$ K (open circles) plotted against $(T/T_c)^2$. Results for UBe_{13} (Ref. 16), assuming $\lambda(0) = 4200$ and 8000 Å, are also shown (dashed lines).

previous study.¹⁰

Comparative high-field (18 kG) measurements were also conducted on a fully stoichiometric sintered $\text{YBa}_2\text{Cu}_3\text{O}_7$ sample (dc-magnetization results are shown in Fig. 1) prepared as described elsewhere.^{11,12} The resulting angle-averaged penetration depth $\langle \lambda(T, \theta) \rangle$ deduced assuming a Gaussian line shape and Eq. (2) is plotted against temperature in Fig. 3(b) and compared to a fit (dashed curve) of Eq. (3) assuming a low-temperature value of $\langle \lambda(0, \theta) \rangle = 1740$ Å. Note that by using Eq. (2), our earlier (3.4 kG) data² give $\langle \lambda(0, \theta) \rangle \approx 1690$ Å; the slight increase in the penetration depth with field follows from the field dependence of the vortex core density.¹³ In view of possible dirty-limit corrections,¹⁴ anisotropy, and flux-pinning¹⁵ effects, agreement between the data and Eq. (3) is excellent. The inset shows the relative incremental penetration depth for $T \leq 40$ K (open circles) plotted against $(T/T_c)^2$, and compared to a linear fit (solid line) assuming a zero y intercept. As is evident, these data exhibit a small $(T/T_c)^2$ contribution, well below the corresponding data¹⁶ for UBe_{13} (dashed lines);

the single-crystal data of Fig. 3(a) show even less T^2 dependence. Equally evident is the absence of any measurable linear increase in $\langle \lambda(T, \theta) \rangle$ with T at the lowest temperatures, in contrast to specific-heat measurements¹⁷ which indicated linear terms near $T=0$ in various oxides of copper. Thus, if genuinely present, the excitations probed in the specific-heat experiments do not appear capable of inducing pair breaking in these materials.

To explore the anisotropy of the magnetic penetration depth in $\text{YBa}_2\text{Cu}_3\text{O}_{7-\delta}$, we repeated the measurements with the external field applied at an angle $\theta = \pi/4$ radians with respect to the c axis. The width of the field distribution $\langle |\Delta B|^2 \rangle$ for $\theta = \pi/4$ is compared to the $\theta = 0$ value in the inset of Fig. 3(a). The dashed line in the inset corresponds to the angle-averaged value. Assuming that a simple triangular (or square) vortex lattice continues to exist for $\theta > 0$, and that a single-band description with a diagonal effective-mass tensor is applicable, one can calculate¹⁸ the expected angular dependence of the effective-mass tensor. Representative curves, calculated from Ref. 18 for various values of m_c^*/m_{ab}^* , are shown in the inset of Fig. 3(a) and clearly indicate that the superconductivity in $\text{YBa}_2\text{Cu}_3\text{O}_{7-\delta}$ is strongly anisotropic ($m_c^*/m_{ab}^* \geq 25$), in agreement with critical-field and critical-current density measurements.¹⁹ Correspondingly, the c -axis penetration depth associated with the carrier momentum along the c axis is then $\lambda_c > 7000$ Å. For large anisotropies (i.e., $m_{ab}^*/m_c^* \geq 25$), the angular dependence of $\langle |\Delta B|^2 \rangle$ becomes independent of the effective-mass ratio. In this limiting case, the hard-axis and angle-averaged values of the magnetic penetration depth are related via the expression $\lambda(T, 0) = \langle \lambda(T, \theta) \rangle / 1.23$.¹⁸ Applying this formula to the sintered powder data of Fig. 3(b), then gives $\lambda_{ab}^{\text{powder}} \sim 1415$ Å, in good agreement with the single-crystal result.

In type-II superconductors, the penetration depth is given by the London formula,

$$\lambda(T=0, \theta) \approx \left(\frac{m^*(\theta)c^2}{4\pi\eta_s e^2} \right)^{1/2} = \left(\frac{m^*(\theta)/m_e}{4\pi\eta_s r_e} \right)^{1/2}, \quad (4)$$

where $r_e = e^2/m_e c^2 = 2.82 \times 10^{-5}$ Å is the classical electron radius, η_s is the superfluid carrier density which, for ordinary superconductors at $T=0$, is identical to the normal-state carrier density η , m^* is the effective mass, and m_e is the free-electron mass. According to Eq. (4), the penetration depth is completely determined by the two unknowns, η and m^* . A second fundamental quantity, having a different functional dependence on the same two unknowns, is the Sommerfeld constant γ which, for an isotropic three-dimensional system, can be written as

$$\gamma = k_B^2 \left(\frac{\pi}{3} \right)^{2/3} \frac{m^*}{\hbar^2} \eta^{1/3}, \quad (5a)$$

while, for a stack of two-dimensional systems with spacing Δ between them,

$$\gamma = \frac{\pi}{3} k_B^2 \frac{m^*}{\hbar^2} \frac{1}{\Delta}. \quad (5b)$$

In the absence of information on the anisotropy of the effective mass, Eq. (5a) has generally been used to obtain estimates of m^*/m_e . From the present work, however, it is clear that the m^* relevant for λ is extremely anisotropic, and therefore likely that the same is true for the thermodynamic m^* . Thus, Eq. (5b) is more applicable than Eq. (5a) in determining the extent of the effective-mass renormalization in the high- T_c copper oxides. Assuming that the layer spacing Δ is the mean distance between the square CuO_2 planes in $\text{YBa}_2\text{Cu}_3\text{O}_7$ ($\Delta = 5.85 \text{ \AA}$) and a Sommerfeld constant of $\gamma \approx 10 \text{ mJ}/(\text{mole Cu K}^2)$,²⁰ we find that $m_{ab}^*/m_e \approx 10$. Since η does not appear in Eq. (5b), Δ and γ alone are sufficient to determine the thermodynamic m_{ab}^* which, in this case, agrees with the in-plane effective mass determined from a detailed analysis²¹ of the infrared data for the 60 K ($0.3 \lesssim \delta \lesssim 0.4$) phase. By further assuming that the m^* appearing in Eq. (4) is the same as that in Eq. (5b), and using our value for $\lambda_{ab}(0)$, the carrier density obtained from Eq. (4) is $\eta \approx 1.4 \times 10^{22} \text{ carriers cm}^{-3}$, in good agreement with Hall-effect measurements.²² Before concluding, we emphasize that while quite successful, our calculations of η and m_{ab}^*/m_e are merely approximate, especially in view of the clean-limit assumed and electronic-structure calculations²³ which in-

dicates that at least three bands cross the Fermi level for $\delta = 0$.

To summarize, we have measured the temperature and orientation dependence of the magnetic penetration depth $\lambda(T, \theta)$ for single-crystal $\text{YBa}_2\text{Cu}_3\text{O}_{7-\delta}$ (with $\delta \sim 0.1$). Results are consistent with conventional s -wave pairing, yielding a value of $\lambda(0, 0) = \lambda_{ab}(0) = 1415 \pm 30 \text{ \AA}$ parallel to the basal plane, and an effective-mass anisotropy of $m_c^*/m_{ab}^* \geq 25$. The angle-averaged penetration depth for a fully stoichiometric sample is also shown, using the formalism of Ref. 18, to be consistent with the single-crystal result. The extreme anisotropy of λ suggests that the carriers in $\text{YBa}_2\text{Cu}_3\text{O}_{7-\delta}$ belong to a relatively dense ($\eta_{2d} = \eta\Delta \approx 8 \times 10^{14} \text{ carriers cm}^{-2}$, $1/\sqrt{\eta_{2d}} \approx 3.5 \text{ \AA}$) two-dimensional Fermi liquid with effective mass, $m_{ab}^*/m_e \approx 10$.

The authors thank K. Hoyle and J. Worden for technical assistance. We also express our gratitude to A. T. Fiory, A. Millis, C. M. Varma, and W. Barford for many helpful discussions. Research at TRIUMF is supported by the Natural Sciences and Engineering Research Council of Canada and, through TRIUMF, by the Canadian National Research Council.

*Also at Risø National Laboratory, DK-4000 Roskilde, Denmark.

¹For a survey of the early literature, see T. Forgan, *Nature* **329**, 483 (1987).

²D. R. Harshman *et al.*, *Phys. Rev. B* **36**, 2386 (1987).

³G. Aeppli *et al.*, *Phys. Rev. B* **35**, 7129 (1987); W. J. Kossler *et al.*, *ibid.* **35**, 7133 (1987); F. N. Gygax *et al.*, *Europhys. Lett.* **4**, 473 (1987); R. Wäppling *et al.*, *Phys. Lett. A* **122**, 209 (1987); A. Golnik *et al.*, *ibid.* **125**, 71 (1987); D. W. Cooke *et al.*, *Phys. Rev. B* **37**, 9401 (1988); J. R. Cooper *et al.*, *ibid.* **37**, 638 (1988); E. M. Jackson *et al.*, *Physica C* **152**, 125 (1988); R. Felici *et al.*, *Nature* **329**, 503 (1987); A. Umezawa *et al.*, *Phys. Rev. B* **38**, 2843 (1988); A. T. Fiory *et al.*, *Phys. Rev. Lett.* **61**, 1419 (1988).

⁴L. F. Schneemeyer *et al.*, *Nature* **238**, 601 (1987).

⁵A. Schenck, *Muon Spin Rotation Spectroscopy* (Hilger, Bristol, England, 1985); S. F. J. Cox, *J. Phys. C* **20**, 3187 (1987).

⁶D. R. Harshman *et al.* (unpublished).

⁷E. H. Brandt, *Phys. Rev. B* **37**, 2349 (1988); E. H. Brandt and A. Seeger, *Adv. Phys.* **35**, 189 (1986).

⁸J. Orenstein (private communication); see also, T. Timusk *et al.* (unpublished).

⁹M. Tinkham and R. A. Ferrell, *Phys. Rev. Lett.* **2**, 331 (1959).

¹⁰Y. J. Uemura *et al.*, *Phys. Rev. B* **38**, 909 (1988).

¹¹R. J. Cava *et al.*, *Phys. Rev. Lett.* **58**, 1676 (1987).

¹²R. J. Cava *et al.*, *Nature* **329**, 423 (1987); *ibid.* *Phys. Rev. B* **36**, 5719 (1987).

¹³J. W. Ekin and J. R. Clem, *Phys. Rev. B* **12**, 1753 (1975).

¹⁴A. L. Fetter and P. C. Hohenberg, in *Superconductivity*, edited by R. D. Parks (Dekker, New York, 1969), Chap. 14.

¹⁵P. H. Kes *et al.*, in Proceedings of the Latin American Conference on High- T_c Superconductivity, Rio de Janeiro, Brazil, 1988 (unpublished); J. van den Berg *et al.*, *Physica C* **153-155**, 1465 (1988).

¹⁶D. Einzel *et al.*, *Phys. Rev. Lett.* **56**, 2513 (1986).

¹⁷See, e.g., S. J. Collocott *et al.* *Phys. Rev. B* **36**, 5684 (1987).

¹⁸W. Barford and J. M. F. Gunn, *Physica C* **156**, 515 (1988); A. Baratoff *et al.* (private communication) have also considered flux lattices where the field is not necessarily perpendicular to the basal plane.

¹⁹T. R. Dinger *et al.*, *Phys. Rev. Lett.* **58**, 2687 (1987).

²⁰A. Junod *et al.*, *Physica C* **152**, 50 (1988); S. E. Inderhees *et al.*, *Phys. Rev. Lett.* **60**, 1178 (1988).

²¹G. A. Thomas *et al.*, *Phys. Rev. Lett.* **61**, 1313 (1988).

²²G. S. Grader *et al.*, *Phys. Rev. B* **38**, 844 (1988).

²³L. F. Mattheiss and D. R. Hamann, *Solid State Commun.* **63**, 395 (1987); S. Massidda *et al.*, *Phys. Lett. A* **122**, 198 (1987); J. Yu *et al.*, *ibid.* **122**, 203 (1987).